

Properties of four numerical schemes applied to a nonlinear scalar wave equation with a GR-type nonlinearity

Jakob Hansen¹, Alexei Khokhlov² and Igor Novikov^{1,3,4}

November 14, 2018

Abstract

We study stability, dispersion and dissipation properties of four numerical schemes (Iterative Crank-Nicolson, 3'rd and 4'th order Runge-Kutta and Courant-Fredrichs-Levy Non-linear). By use of a Von Neumann analysis we study the schemes applied to a scalar linear wave equation as well as a scalar non-linear wave equation with a type of non-linearity present in GR-equations. Numerical testing is done to verify analytic results. We find that the method of lines (MOL) schemes are the most dispersive and dissipative schemes. The Courant-Fredrichs-Levy Non-linear (CFLN) scheme is most accurate and least dispersive and dissipative, but the absence of dissipation at Nyquist frequency, if fact, puts it at a disadvantage in numerical simulation. Overall, the 4'th order Runge-Kutta scheme, which has the least amount of dissipation among the MOL schemes, seems to be the most suitable compromise between the overall accuracy and damping at short wavelengths.

¹Niels Bohr Institute, Blegdamsvej 17, DK-2100 Copenhagen, Denmark

²Department of Astronomy and Astrophysics, The University of Chicago, 5640 Ellis Avenue, Chicago, IL 60637, USA

³NORDITA, Blegdamsvej 17, DK-2100 Copenhagen, Denmark

⁴Astro Space Center of P.N. Lebedev Physical Institute, Profsoyuznaja 83/32, Moscow 118710, Russia

1 Introduction

The area of numerical relativity is very complex with many factors influencing the calculations. Due to this complexity, choosing a best numerical scheme for solving problems in general relativity (GR) may be of particular importance in order to have a long term stability and to minimize truncation errors. At the same time, problems in numerical relativity usually demand a large amount of computational resources. Hence it is also desirable to choose a scheme which best exploits the available computer power at any given time, i.e. provides accurate results with a minimal number of operations.

First and foremost the scheme needs to be numerically stable, but in addition to this basic (but not always trivially established) property, there are a number of other features, such as accuracy, dissipation and dispersion properties, which may have important impacts on the numerical solutions as well.

The purpose of this paper is to investigate numerical properties (in particular dispersion, stability and dissipation) of some numerical schemes which can be used to solve GR type equations, allowing users of these schemes to estimate potential pitfalls and limitations of the schemes. The schemes that are being analyzed are the iterative Crank-Nicolson scheme (ICN), the third and fourth order Runge-Kutta schemes (RK3 and RK4) and a nonlinear version of the classical Courant-Friedrichs-Levy scheme (CFLN). A unique aspect of numerical GR is that the integration may be affected not only by stability of the scheme, but also by constraint and gauge instabilities which are intrinsic to the equations themselves. In order to separate these effects from the stability of the schemes and to investigate strengths and weaknesses of the different schemes, we want to apply the schemes to simpler scalar wave equations. Numerical schemes are usually analyzed by their application to the standard linear scalar wave equation (e.g. [1], [2]) however, they are usually applied to solve nonlinear problems. By use of a classical Von Neumann analysis, we analyze properties of the schemes applied to both the standard scalar linear wave equation and to a nonlinear scalar wave equation, which is designed to mimic some properties of the nonlinear terms in the Einstein equations. By this we hope to expand our knowledge of the behavior of the schemes in a regime which is closer to the computational reality of numerical GR than a sole analysis of the schemes in the fully linear regime. The non-linear wave equation, a perturbation analysis of it and the numerical schemes are presented in section 2. The results from the Von Neumann analysis of the schemes applied to the scalar linear and nonlinear wave equations are presented in section 3 and 4 respectively. To support the analytic results, numerical results are presented in section 5.

2 Formulation of the problem

In this section we present the numerical schemes which we will analyze in subsequent sections, the non-linear scalar wave equation to which we will apply the schemes and the method by which we will be analysis the schemes.

2.1 A Non-linear Wave Equation

Consider the following scalar, quasi-linear, hyperbolic partial differential equation of two independent variables, t and x ([3]):

$$\frac{\partial^2 g}{\partial t^2} = \frac{\partial^2 g}{\partial x^2} - \frac{1}{g} \left(\frac{\partial g}{\partial t} \right)^2 \quad (2.1)$$

or cast into first order form:

$$\begin{aligned} \frac{\partial g}{\partial t} &= K \\ \frac{\partial K}{\partial t} &= \frac{\partial^2 g}{\partial x^2} - \frac{(K)^2}{g} \end{aligned} \quad (2.2)$$

This equation is essentially the standard scalar wave equation with an added non-linear term. The equation is interesting because the non-linear term mimics part of the non-linearities present in GR equations. This can be seen by recalling that the structure of a Ricci tensor R_{ab} is $R \sim \sum \partial\Gamma + \sum \Gamma\Gamma$, where Christoffel symbols $\Gamma \sim g^{-1}\partial g$, and g is the metric. Thus R_{ab} can be represented as a sum of the terms $R \sim \sum g^{-1}\partial^2 g + \sum g^{-2}(\partial g)^2$. Equation (2.1) thus mimics a type of non-linearity present in GR equations $R_{ab} = 0$. Especially equations (2.2) resembles the evolutionary part of GR equation in a standard ADM 3+1 form (with zero shift and constant lapse). We expect that in order to successfully apply the schemes to GR equations they must be applicable equation (2.1).

Equation (2.1) possesses a large number of non-trivial solutions [3]. For test purposes we use two particular analytical solutions to this equation: A spatial constant solution:

$$g(t) = \sqrt{C_1 + C_2 \cdot t}, (C_1 + C_2 \cdot t \geq 0).^1 \quad (2.3)$$

and an exponential solution:

$$g(x, t) = \exp \left(\pm \sqrt{C} \cdot x \pm \sqrt{\frac{C}{2}} \cdot t \right), (C \geq 0, \pm \text{ signs independent})^2. \quad (2.4)$$

2.2 Perturbation analysis

We wish to analyze the analytical behavior of small amplitude perturbations of solutions (2.3) and (2.4).

Let $g_0(x, t)$ be a base solution of equation (2.1) and let $g_0 + \tilde{g}$ be a perturbed solution, with $|\tilde{g}| \ll |g_0|$. We linearize (2.1) around g_0 and obtain a linear equation for the perturbations

$$\frac{\partial^2 \tilde{g}}{\partial t^2} = \frac{\partial^2 \tilde{g}}{\partial x^2} - 2 \left(\frac{1}{g_0} \frac{\partial g_0}{\partial t} \right) \frac{\partial \tilde{g}}{\partial t} + \left(\frac{1}{g_0} \frac{\partial g_0}{\partial t} \right)^2 \tilde{g} \quad (2.5)$$

¹ $g(t) = -\sqrt{C_1 + C_2 \cdot t}$ is naturally also a solution but since we are trying to mimic some features of the Einstein equations, g (which mimics the 3-metric of the general relativity) cannot be negative. This is also why we require $C_1 + C_2 \cdot t \geq 0$ as we would otherwise obtain complex solutions which would be unphysical.

² C cannot be negative as this would create complex solutions (see previous footnote).

or

$$\frac{\partial^2 \tilde{g}}{\partial t^2} = \frac{\partial^2 \tilde{g}}{\partial x^2} - 2A \frac{\partial \tilde{g}}{\partial t} + A^2 \tilde{g} \quad (2.6)$$

where

$$A \equiv \frac{1}{g_0} \frac{\partial g_0}{\partial t} \quad (2.7)$$

Consider perturbations of the form:

$$\tilde{g} \propto e^{I\omega t - Ikx}. \quad (2.8)$$

where $I = \sqrt{-1}$. Then the dispersion relation is

$$\omega^2 = k^2 + 2AI\omega - A^2. \quad (2.9)$$

Substituting $\omega = \omega_R + I\omega_I$ into equation (2.9) and separating real and imaginary parts we obtain:

$$2I\omega_R\omega_I = 2IA\omega_R \quad (2.10)$$

$$\omega_R^2 - \omega_I^2 = k^2 - 2A\omega_I - A^2 \quad (2.11)$$

From (2.10) it follows that $\omega_I = A$, hence the growth rate of a perturbation $\tilde{g} \propto e^{I\omega_I t}$ is

$$\tilde{g} \propto e^{-At}. \quad (2.12)$$

We see that a base solution is stable if $A \geq 0$ and otherwise it is unstable. Hence growing solutions are stable and decaying solutions are unstable.

Due to a local linearization involved in the above analysis, the conclusion is strictly valid for perturbations with high wave numbers $k = \frac{2\pi}{\lambda}$ compared to the base solutions, and only if the growth rate is \gg then that of the base solution. By looking at the spatial constant base solution (2.3), perturbed by a spatial constant perturbation ($k = 0$), we can estimate the behavior of spatial constant or very long wavelength perturbations.

Consider a spatial constant base solution (2.3) perturbed by a small spatially constant perturbation: $g(t) = g_0(t) + \tilde{g}(t)$. Then equation (2.5) simplifies to an ordinary differential equation which can be solved to yield:

$$\tilde{g}(t) = \pm \frac{K}{2} \left(\frac{\sqrt{2}}{g_0(t)} + \frac{g_0(t)}{\sqrt{2}} \right) \quad (2.13)$$

where K is an arbitrary integration constant. From (2.13) we see that for growing base solutions (i.e. positive C_2 in (2.3)) the second term is growing proportionally to the base solution, while the first term is decaying inversely proportionally to the base solution, hence the relative error is decreasing towards a constant value proportional to K . That is, the perturbation is growing but it is not unstable. If the base solution is decaying (i.e. negative C_2 in (2.3)), the first term increases rapidly as $g_0(t) \rightarrow 0$ and the solution becomes unstable as the relative error grows unbounded.

2.3 The Numerical Schemes

The four schemes that we are investigating are

- Iterative Crank-Nicolson
- 3'rd order Runge-Kutta
- 4'th order Runge-Kutta
- Courant-Friedrichs-Levy Nonlinear

The first three schemes are based on the method of lines approach [4], while the Courant-Friedrichs-Levy Nonlinear scheme is based on the classic central-difference, second-order explicit scheme introduced in 1928 by Courant, Friedrichs and Levy [5]. The schemes are defined as follows:

2.3.1 The Iterative Crank-Nicolson scheme

The iterative Crank-Nicolson scheme (ICN) is an explicit, iterative scheme which was developed by Matt Choptuik from the classic implicit Crank-Nicolson scheme [6], [7]. To solve equation (2.2), we define the ICN-scheme as follows. First the iteration process is initiated:

$$\begin{aligned} K_i^{(1)} &= K_i^n + \Delta t (\delta^2 (g_i^n) + NLT (g_i^n, K_i^n)) \\ g_i^{(1)} &= g_i^n + \Delta t \cdot K_i^n \end{aligned} \tag{2.14}$$

where $\delta^2(g_i^n) = \frac{g_{i-1}^n - 2g_i^n + g_{i+1}^n}{\Delta x^2}$ is the centered second order accurate finite difference approximation to the second order spatial derivative, g_i^n and K_i^n are determined at mesh points $x_i = i\Delta x$, $t^n = n\Delta t$ and $NLT(g_i^n, K_i^n)$ is the non-linear term (i.e for eq. (2.2) $NLT(g_i^n, K_i^n) = \frac{(K_i^n)^2}{g_i^n}$). The scheme is then iterated:

$$\begin{aligned} K_i^{(j)} &= K_i^n + \Delta t \left(\delta^2 \left(\frac{g_i^{(j-1)} + g_i^n}{2} \right) + NLT \left(\frac{g_i^{(j-1)} + g_i^n}{2}, \frac{K_i^{(j-1)} + K_i^n}{2} \right) \right) \\ g_i^{(j)} &= g_i^n + \Delta t \left(\frac{K_i^{(j-1)} + K_i^n}{2} \right) \end{aligned} \tag{2.15}$$

$j \in [2, j_{max}]$), and finally the dependent variables at the next time step are:

$$\begin{aligned} K_i^{(n+1)} &= K_i^{(j_{max})} \\ g_i^{(n+1)} &= g_i^{(j_{max})} \end{aligned} \tag{2.16}$$

As shown in [1] and [2], the optimal number of iterations, for the scalar wave equation is $j_{max} = 3^1$, which is the scheme that we will investigate in this paper. This scheme can be shown to be second order accurate in both time and space by a Taylor series expansion [1],[2].

¹Note that different authors count the number of iterations in different ways, some do not count the first step as an iteration and hence state that the optimal number of iterations is 2.

2.3.2 The 3'rd order Runge-Kutta scheme

To solve eq. (2.2), the 3'rd order Runge-Kutta scheme (RK3) is defined as follows [8]:

$$\begin{aligned} K_i^{n+1} &= K_i^n + \frac{K_i^{(1)} + 4K_i^{(2)} + K_i^{(3)}}{6} \\ g_i^{n+1} &= g_i^n + \frac{g_i^{(1)} + 4g_i^{(2)} + g_i^{(3)}}{6} \end{aligned} \quad (2.17)$$

where

$$\begin{aligned} K_i^{(1)} &= \Delta t [\delta^2 (g_i^n) + NLT (g_i^n, K_i^n)] \\ g_i^{(1)} &= \Delta t [K_i^n] \\ K_i^{(2)} &= \Delta t \left[\delta^2 \left(g_i^n + \frac{g_i^{(1)}}{2} \right) + NLT \left(g_i^n + \frac{g_i^{(1)}}{2}, K_i^n + \frac{K_i^{(1)}}{2} \right) \right] \\ g_i^{(2)} &= \Delta t \left[K_i^n + \frac{K_i^{(1)}}{2} \right] \\ K_i^{(3)} &= \Delta t \left[\delta^2 \left(g_i^n - g_i^{(1)} + 2g_i^{(2)} \right) + NLT \left(g_i^n - g_i^{(1)} + 2g_i^{(2)}, K_i^n - K_i^{(1)} + 2K_i^{(2)} \right) \right] \\ g_i^{(3)} &= \Delta t \left[K_i^n - K_i^{(1)} + 2K_i^{(2)} \right] \end{aligned} \quad (2.18)$$

This scheme can be shown to be second order accurate in space and third order accurate in time by a Taylor series expansion.

2.3.3 The 4'th order Runge-Kutta scheme

To solve eq. (2.2) the 4'th order Runge-Kutta scheme (RK4) is defined as follows [8]:

$$\begin{aligned} K_i^{n+1} &= K_i^n + \frac{K_i^{(1)} + 2K_i^{(2)} + 2K_i^{(3)} + K_i^{(4)}}{6} \\ g_i^{n+1} &= g_i^n + \frac{g_i^{(1)} + 2g_i^{(2)} + 2g_i^{(3)} + g_i^{(4)}}{6} \end{aligned} \quad (2.19)$$

where

$$\begin{aligned}
K_i^{(1)} &= \Delta t \left[\delta^2 (g_i^n) + NLT (g_i^n, K_i^n) \right] \\
g_i^{(1)} &= \Delta t [K_i^n] \\
K_i^{(2)} &= \Delta t \left[\delta^2 \left(g_i^n + \frac{g_i^{(1)}}{2} \right) + NLT \left(g_i^n + \frac{g_i^{(1)}}{2}, K_i^n + \frac{K_i^{(1)}}{2} \right) \right] \\
g_i^{(2)} &= \Delta t \left[K_i^n + \frac{K_i^{(1)}}{2} \right] \\
K_i^{(3)} &= \Delta t \left[\delta^2 \left(g_i^n + \frac{g_i^{(2)}}{2} \right) + NLT \left(g_i^n + \frac{g_i^{(2)}}{2}, K_i^n + \frac{K_i^{(2)}}{2} \right) \right] \\
g_i^{(3)} &= \Delta t \left[K_i^n + \frac{K_i^{(2)}}{2} \right] \\
K_i^{(4)} &= \Delta t \left[\delta^2 \left(g_i^n + g_i^{(3)} \right) + NLT \left(g_i^n + g_i^{(3)}, K_i^n + K_i^{(3)} \right) \right] \\
g_i^{(4)} &= \Delta t \left[K_i^n + K_i^{(3)} \right]
\end{aligned} \tag{2.20}$$

This scheme can be shown to be second order accurate in space and fourth order accurate in time by a Taylor series expansion.

2.3.4 Crank-Friedrichs-Levy Nonlinear scheme (CFLN)

Another approach to solving eq.(2.2) numerically is to notice that without the non-linear term, equation (2.2) is a scalar wave equation which can be solved by the classic explicit scheme by Courant, Friedrichs and Levy [5](see also cp. 10 in [7]):

$$\frac{g_i^{n+1} - 2g_i^n + g_i^{n-1}}{\Delta t^2} = \frac{g_{i+1}^n - 2g_i^n + g_{i-1}^n}{\Delta x^2} \tag{2.21}$$

We can cast this scheme into a first order form:

$$\begin{aligned}
K_i^{n+\frac{1}{2}} &= K_i^{n-\frac{1}{2}} + \Delta t (\delta^2 (g_i^n)) \\
g_i^{n+1} &= g_i^n + \Delta t K_i^{n+\frac{1}{2}}
\end{aligned} \tag{2.22}$$

Now, in order to use this scheme as a basis for solving equation (2.2), we must add a term to evolve the non-linear part, moreover, we wish to do this with second-order accuracy at the grid points (x_i, t^n) to ensure overall second-order accuracy of the scheme. We do this by evaluating the non-linear term using the following predictor-corrector style approach [3]:

$$\begin{aligned}
\tilde{K}_i^{n+\frac{1}{2}} &= K_i^{n-\frac{1}{2}} + \Delta t \left(\delta^2 (g_i^n) + NLT (g_i^n, K_i^{n-\frac{1}{2}}) \right) \\
K_i^{n+\frac{1}{2}} &= \tilde{K}_i^{n+\frac{1}{2}} + \frac{\Delta t}{2} \left(NLT (g_i^n, K_i^{n-\frac{1}{2}}) + NLT (g_i^n, \tilde{K}_i^{n+\frac{1}{2}}) \right) \\
g_i^{n+1} &= g_i^n + \Delta t K_i^{n+\frac{1}{2}}
\end{aligned} \tag{2.23}$$

This scheme can be shown to be second order accurate in both space and time by a Taylor series expansion. An advantage of the scheme is that the second-order accuracy is achieved with a relatively small number of right hand side operations, to calculate one time step CFLN requires 2 evaluations of the non-linear terms, compared to 3 evaluations required for the ICN and RK3 schemes and 4 evaluations required for the RK4 scheme. It is also noted that the scheme is staggered in time, i.e. initial values are required at points $g_{j-i,j,j+1}^n, K_i^{n-\frac{1}{2}}$.

2.4 The Von Neumann analysis

To investigate the properties of the numerical schemes we use a Von Neumann analysis following a standard approach [7],[9]: All the schemes can be represented by the following evolution operator:

$$U_{j,l}^{n+1} = S_{j,l}^n(U_{j',l'}^n) \quad (2.24)$$

where $U_{j,l}^n$ is a set of dynamical variables, n and j are temporal and spatial indices respectively and l enumerates the dynamic variables. In our case, the operator $S_{j,l}^n$ may depend on all components of $U_{j',l'}^n$ at grid points ($j = j - 1, j, j + 1$) corresponding to a time layer n (or a combination of n and $n - \frac{1}{2}$ in the staggered case of CFLN scheme).

Perturbing $U_{j,l}^n$ as

$$U_{j,l}^n = \hat{U}_{j,l}^n + \delta U_{j,l}^n, \quad (2.25)$$

where $\hat{U}_{j,l}^n$ is the background solution, substituting equation (2.25) into (2.24) and doing a Taylor-expansion, we obtain

$$\delta U_{j,l}^{n+1} = \sum_{j',l'} \frac{\partial S_{j,l}^n}{\partial \hat{U}_{j',l'}^n} \delta U_{j',l'}^n + O\left((\delta U_{j',l'}^n)^2\right) \quad (2.26)$$

Assuming a perturbation of the form

$$\delta U_{j,l}^n = \xi_l^n e^{-Ij\Delta xk}, \quad (2.27)$$

where $0 < k < \frac{\pi}{\Delta x}$ is the perturbation wave number and $I = \sqrt{-1}$, and substituting (2.27) into (2.26) we obtain

$$\xi_l^{n+1} \approx \sum_{j',l'} \frac{\partial S_{j,l}^n}{\partial U_{j',l'}^n} \xi_{l'}^n e^{I(j-j')\Delta xk} \equiv G_{j,l,l'}^n \xi_{l'}^n \quad (2.28)$$

The *amplification matrix* $G_{j,l,l'}^n$

$$G_{j,l,l'}^n = \sum_{j'} \frac{\partial S_{j,l}^n}{\partial U_{j',l'}^n} e^{I(j-j')\Delta xk} \quad (2.29)$$

holds information about properties of the numerical schemes.

For a linear finite difference equation, the amplification matrix only depends on the discretization parameters Δt , Δx and the wave number k , and needs to be calculated only once in order to know properties of the scheme at all times and grid points. For non-linear schemes the

amplification matrix depends on $\hat{U}_{j,t}^n$ and must in principle be evaluated at *all* spatial points and at *all* points in time.

The generally complex eigenvalues of the amplification matrix, λ_i , hold information about the amplification and speed of a given perturbation for a single time step which can be extracted by calculating the modulus and argument of the eigenvalues respectively. The classic condition for numerical stability is that the spectral radius (i.e. the largest modulus of the eigenvalues) of the amplification matrix is less than or equal to 1 for all wave numbers [7], however this excludes the possibility of growing exponential solutions. A less strict stability requirement (the Von Neumann stability criterion) which allows for exponentially growing solutions is that the eigenvalues must satisfy

$$|\lambda| \equiv \max_i |\lambda_i| \leq 1 + O(\Delta t) \tag{2.30}$$

for all k [7]. In this paper, we will refer to the spectral radius $|\lambda|$ as the amplification factor. We presents amplification factors as a function of $k \cdot \Delta x$ which runs in the range $k \cdot \Delta x \in [0, \pi]$ with $k \cdot \Delta x = \pi$ corresponding to the Nyquist frequency.

It should be noted that due to the local linearization involved in calculating the eigenvalues for non-linear schemes, the Von Neumann analysis is only locally valid. This also means that the analysis cannot be trusted for non-local wave modes, i.e. small wave numbers. However, we *are* most interested in high wave numbers, as experience tells us that numerical instabilities usually arises first at the Nyquist frequencies. Hence for analyzing the stability of a scheme one searches for conditions under which equation (2.30) is valid, focusing on the Nyquist frequency, which usually reduces to a restriction on the relationship between Δt and Δx , known as the Courant number $\alpha = \frac{\Delta x}{\Delta t}$.

3 The linear scalar wave equation

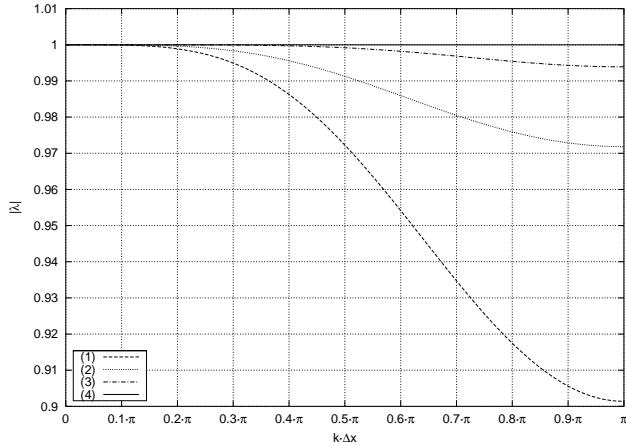
Before studying the non-linear schemes, we briefly summarize stability, dissipation and dispersion properties of the schemes applied for a scalar linear wave equation

$$\frac{\partial^2 g(x, t)}{\partial t^2} = \frac{\partial^2 g(x, t)}{\partial x^2} \tag{3.1}$$

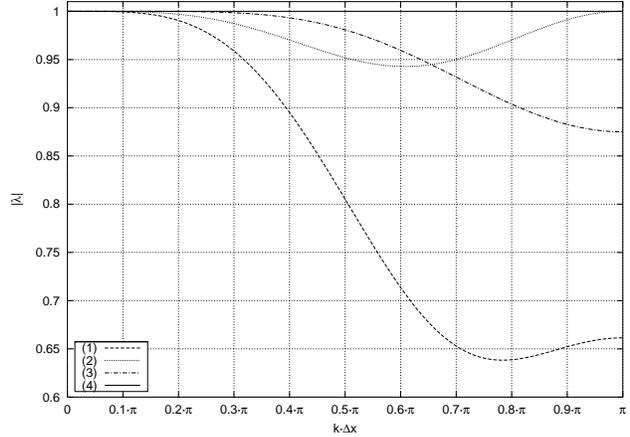
Table 3 shows which Courant intervals satisfies the Von Neumann stability criterion (2.30) for the Nyquist frequency as calculated by a Von Neumann analysis in the limit $\Delta t \rightarrow 0$.

Scheme	Stable Courant interval
ICN	$0 < \alpha < 1$
RK3	$0 < \alpha < \sqrt{\frac{3}{4}}$
RK4	$0 < \alpha < \sqrt{2}$
CFLN	$0 < \alpha < 1$

Table 1: Courant intervals which satisfies the Von Neumann stability criterion (2.30) for the linear wave equation (3.1)



(a) Courant number $\alpha = 0.50$



(b) Courant number $\alpha = \sqrt{0.75}$

Figure 1: Amplification factor as a function of $k \cdot \Delta x$ at Courant number a) $\alpha = 0.50$ and b) $\alpha = \sqrt{0.75}$, respectively, for the 4 schemes investigated. Legend is (1) = ICN, (2) = RK3, (3) = RK4 and (4) = CFLN.

Figure 1 shows the amplification factors as a function of $k \cdot \Delta x$ for Courant numbers $\alpha = 0.50$ and $\alpha = \sqrt{0.75}$ respectively, the latter corresponds to the maximal stable Courant number for the RK3 scheme (cf. table 3). These figures are representative of the dissipative behavior of the four schemes. The plot (and all plots in this section) is valid for all choices of Δx .

For zero wave numbers all schemes are non-dissipative, but with increasing wave numbers and increasing Courant numbers the method of lines schemes shows monotonically increasing dissipation, with ICN being the most dissipative scheme followed by the RK3 and RK4 scheme respectively. For very high wave numbers the dissipation for the method of lines schemes shows a non-monotonic behavior as can be seen by comparing figures 1. We see that the ICN scheme is still, generally, the most dissipative scheme, but as Courant numbers are increased towards the stable limit, the dissipation at the Nyquist frequency vanishes and the maximal dissipation is seen for smaller wave numbers. Figure 2 shows the dissipative behavior of the schemes at the Nyquist frequency as a function of Courant number. This shows how the Nyquist frequency has maximal dissipation at around $\alpha \approx 0.8 \cdot \alpha_{max}$ (where α_{max} is the maximal stable Courant number for the corresponding scheme), after which the dissipation at the Nyquist frequency goes to zero just before numerical instability sets in.

The CFLN scheme, in contrast, is completely non-dissipative for all wave numbers for all stable Courant numbers.

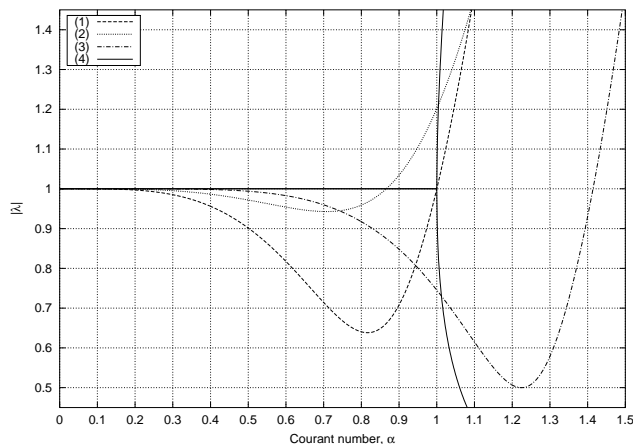


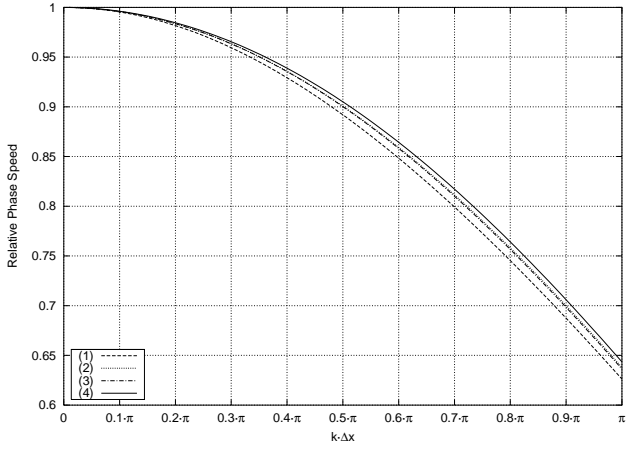
Figure 2: Largest eigenvalues at the Nyquist frequency ($k\Delta x = \pi$) as function of Courant numbers for the 4 schemes investigated. Legend is (1) = ICN, (2) = RK3, (3) = RK4 and (4) = CFLN.

Figure 3 compares the dispersion errors for the four schemes for various Courant numbers as calculated from an Von Neumann analysis for equation (3.1). For small Courant numbers (fig. 3(a)), it is seen that the schemes behaves quite similarly (in fact, for $\alpha \rightarrow 0$ the dispersion errors for the four schemes converge to the same line), but a closer examination shows that the CFLN scheme has the smallest dispersion error, then follows the RK3 and RK4 schemes respectively and finally the ICN scheme which exhibits the largest dispersion errors. Also, dispersion errors are largest for large wave numbers and going to zero in the limit $k \rightarrow 0$ for all schemes.

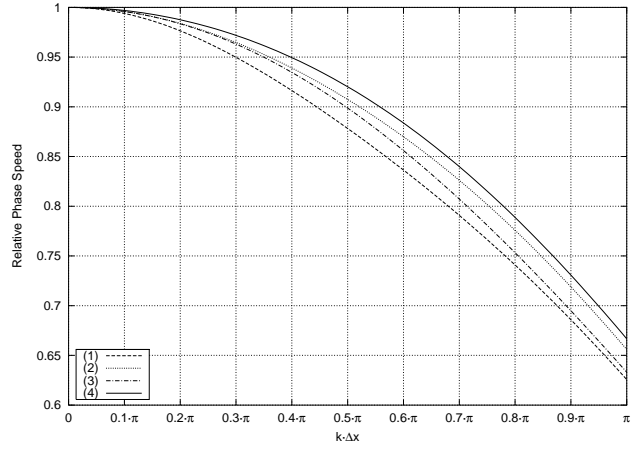
The dispersion errors for the ICN and RK4 schemes are increased monotonically for increasing Courant numbers at smaller wave numbers, while the dispersion errors for these schemes show some non-monotonic behavior at high wave numbers. As can be seen from figure 3(d), the ICN scheme in the limit of $\alpha = 1.00$ exhibits positive dispersion errors for high wave numbers, i.e. the numerical solution is propagating faster than the analytic solution¹.

The dispersion errors for the RK3 and CFLN schemes conversely are minimized for their respective maximal stable Courant numbers. The CFLN scheme in this limit has zero dispersion errors, while the RK3 still has a non-vanishing (but minimized) dispersion error.

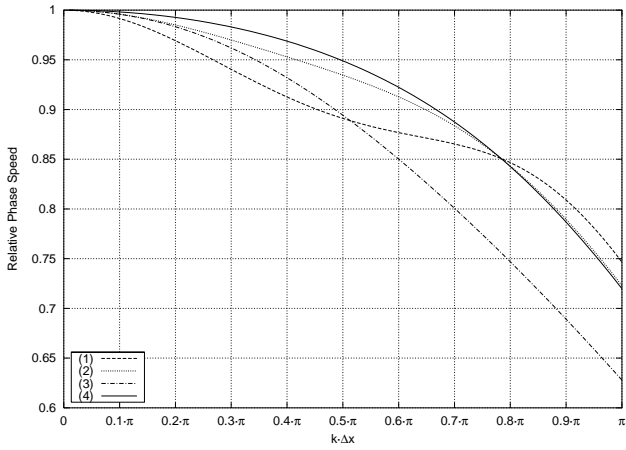
¹However, this is unlikely to be of numerical importance due the high damping for ICN in the high wave number / high Courant number limit.



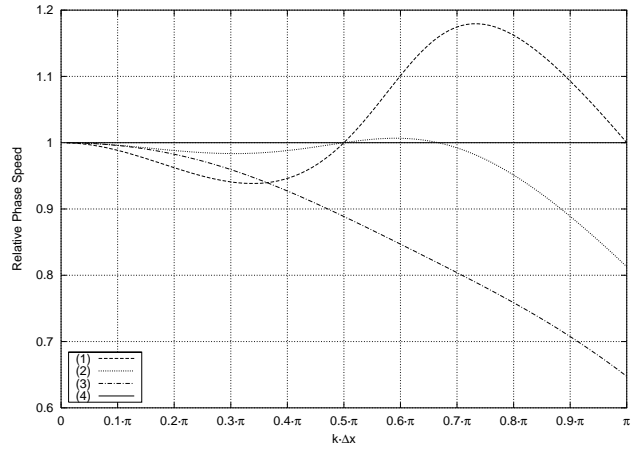
(a) Courant number $\alpha = 0.25$



(b) Courant number $\alpha = 0.50$



(c) Courant number $\alpha = 0.75$

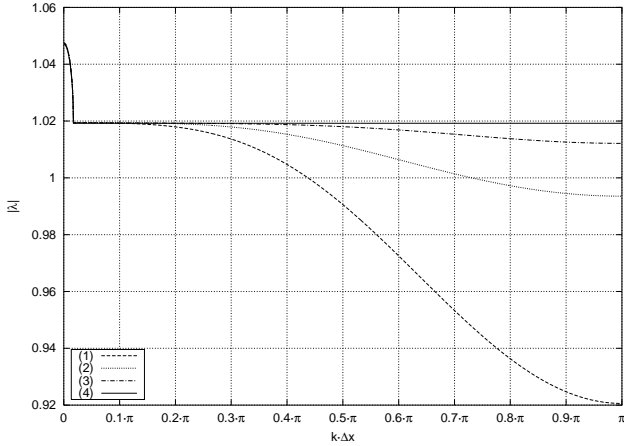


(d) Courant number $\alpha = 1.00$

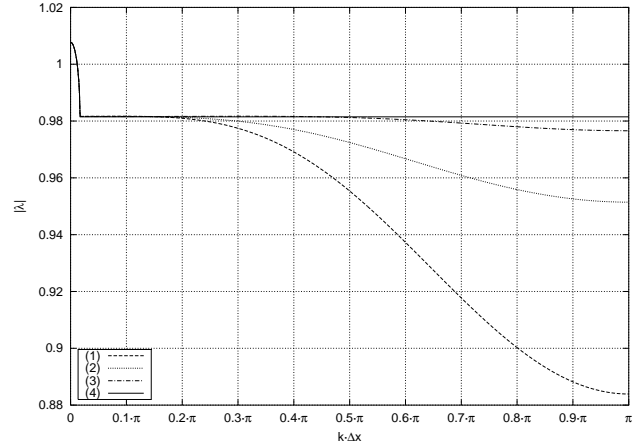
Figure 3: Wave speeds for the four schemes for various Courant numbers relative to the analytic wave speed. Legend is (1) = ICN, (2) = RK3, (3) = RK4 and (4) = CFLN.

4 Von Neumann stability analysis of the non-linear wave equation

We are interested in the behavior of the schemes in the non-linear regime. In this section we present the results of a Von Neumann stability analysis of the four schemes applied to a local linearization of the non-linear wave equation, equation (2.2), presented in section 2.1.



(a) Decaying solution (2.3).



(b) Growing solution (2.3).

Figure 4: Amplification factors for solution (2.3) as a function of $k \cdot \Delta x$. (a) is decaying ($C_2 = -1$) and (b) is growing ($C_2 = 1$). Courant number is $\alpha = 0.5$ and $\Delta x = \frac{\pi}{16}$. Legend is (1) = ICN, (2) = RK3, (3) = RK4 and (4) = CFLN.

4.1 The spatial constant solutions

Figure 4 shows a typical plot of amplification factors versus $k \cdot \Delta x$ for the spatially constant solution (2.3) of equation (2.2) for decaying and growing solutions respectively, for the four schemes. Solution parameters are $C_1 = 2$ for both plots and $C_2 = -1$ and $C_2 = 1$ for figure 4(a) and 4(b) respectively. From the perturbation analysis in subsection 2.2 we expect to observe an amplification for all wave numbers when solution (2.3) is decaying. For growing solutions we expect to see a more modest amplification at small wave numbers and damping at higher wave numbers. Looking at figures 4, we observe that at small wave numbers, all schemes agree with this prediction, i.e. we see a strong amplification at small wave numbers for the decaying solution and a smaller amplification for the growing solution. At high wave numbers the CFLN scheme agrees well with the perturbation analysis and we see an amplification at the Nyquist frequency, while the method of lines schemes all shows various degrees of damping, consistent with the results from section 3. The amount of damping is dependent on the Courant number as in the linear case, but also upon the spatial step size, Δx . By choosing a smaller Δx , for a fixed Courant number, Δt decreases proportionally, by which any amplification also becomes smaller. However, with the amplification factor moving closer to $|\lambda| = 1$, the damping for the method of lines schemes are shifted proportionally, i.e. the method of lines schemes may go from showing amplificative behavior to damping behavior at the Nyquist frequency, with the choice of a smaller Δx . We see this effect in figure 4(a) for the ICN scheme. If we for the same solution had chosen a sufficiently small Δx , the other method of lines schemes would also have shown damping behavior at the Nyquist frequency. The qualitative behavior of the CFLN scheme, in contrast, is unaffected by the choice of Δx for reasonably small Δx . For very large Δx , all the schemes shows abnormal behavior which is caused by the fact that the base solution in this case

changes much more rapid then the temporal resolution allows for.

4.2 The exponential solutions

Figure 5 shows a typical plot of the amplification factors for the four schemes under investigation for the exponentially growing and decaying solution (2.4) to equation (2.2) as a function of $k \cdot \Delta x$ with solution parameter $C = 1$. We see that the plots are very similar to figures 4. For the decaying solution (figure 5(a)) we see that CFLN is an amplificative scheme whereas the method of lines schemes displaying certain amount of dumping. We note that in order to reproduce a correct behavior of perturbed analytic solutions the scheme must have the amplification number greater than one. However, in numerical simulations it may be better to dump growing large wave number (short wavelength) perturbations instead of trying to faithfully reproduce them.

For small wave numbers both the decaying and growing solutions are indicating amplificative behavior. We note that solution (2.4) is spatially dependent, hence the spatially constant perturbation analysis from subsection 2.2 is not valid in this regime. Nevertheless, comparing with figures 4 where we see (and expect) the same behavior it seems plausible that the amplificative behavior seen in the figures is an expected behavior.

As a closing remark to this section, we note that all schemes and solutions has been tested in the limit $\Delta t \rightarrow 0$ to investigate the stability properties of the schemes in the non-linear regime and we have found that all schemes agree with the stability intervals for the linear case (table 3) for all solutions.

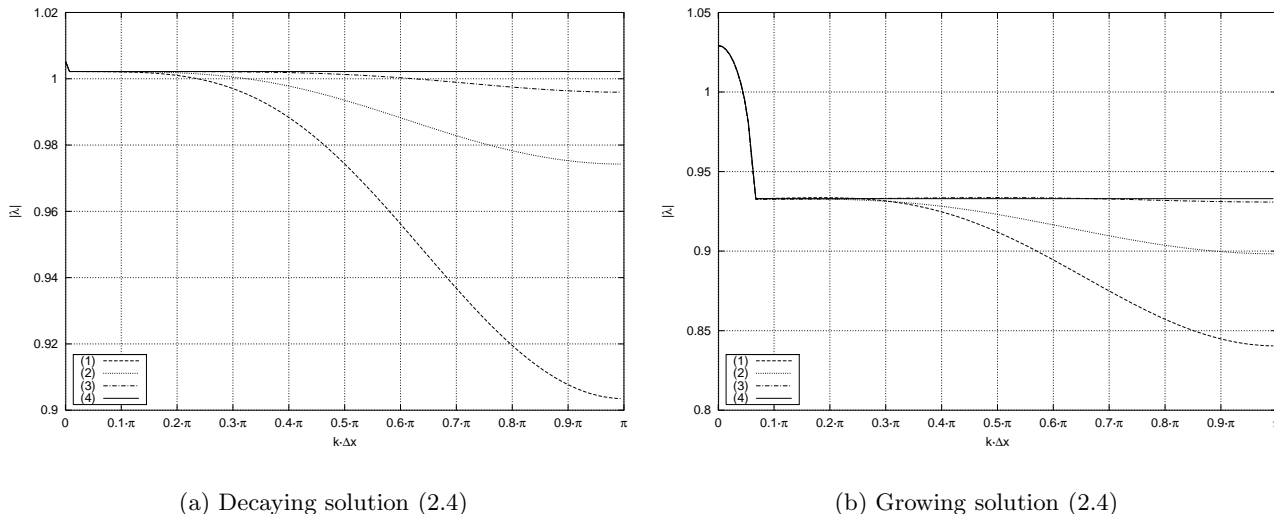


Figure 5: *Amplification factors for solution (2.4) as a function of $k \cdot \Delta x$. (a) is decaying and (b) is growing. Courant number is $\alpha = 0.5$, $\Delta x = \frac{\pi}{16}$ and $C = 1$. Legend is (1) = ICN, (2) = RK3, (3) = RK4 and (4) = CFLN.*

5 Numerical Tests

We have done numerical testings to verify the analytic results presented in the preceding sections. Figure 6 shows the convergence of solution (2.3) to equation (2.2). Plotted on the vertical axis is the absolute error of the central point in the domain between a simulation with the spatial step specified on the horizontal axis and a reference simulation. The reference simulation is a high resolution simulation with a resolution twice that of the leftmost point in the plot. The constants in solution (2.3) were set to $C_1 = 2$ and $C_2 = -1$, the simulations were run for a time $t = \pi/4$ in a domain of size 2π and the Courant number of the simulations was fixed at $\alpha = 0.50$.

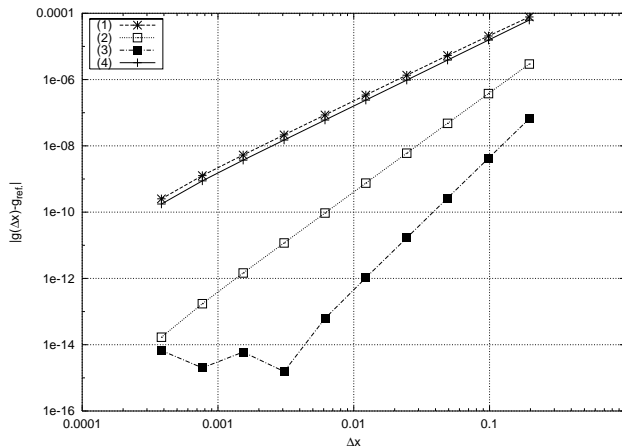


Figure 6: Absolute error between simulation at specified Δx vs. simulation at $\Delta x = \frac{\pi}{2^{14}}$ for Courant number $\alpha = 0.50$. Legend is (1) = ICN, (2) = RK3, (3) = RK4 and (4) = CFLN.

From the figure we see that the CFLN and ICN schemes are showing second order convergence, the RK3 scheme shows third order convergence. The RK4 scheme shows fourth order convergence at large Δx , but flattens out a around 10^{-15} and for small step sizes. The flattening is caused by machine precision errors affecting the solutions. The convergence rates are what should be expected for spatially constant solutions. This solution does not introduce any truncation errors associated with spatial discretization. The figure thus shows convergence rates in agreement with the truncation error due to the temporal discretization of the schemes (second order CFLN and ICN, third order RK3, and fourth order RK4). Identical convergence tests for the exponential solutions (2.4) shows second order convergence for all schemes due to the second order spatial finite difference operator we have used in the schemes to calculate spatial derivatives.

To test analytic predictions of the behavior of a perturbed solution we have made numerical tests of base solutions perturbed by small amplitude sinusoidal perturbations, $g(x, t) = g_0(x, t) + \tilde{g}(x, t, k)$, with wave number k . Figure 7 is identical to figure 6, except that now base solution (2.3) is perturbed by a moving sinusoidal wave with wave number of $k = 16$ (corresponding to the Nyquist frequency for the rightmost point) and initial amplitude $A_0 = 10^{-6}$, all other parameters are as for figure 6.

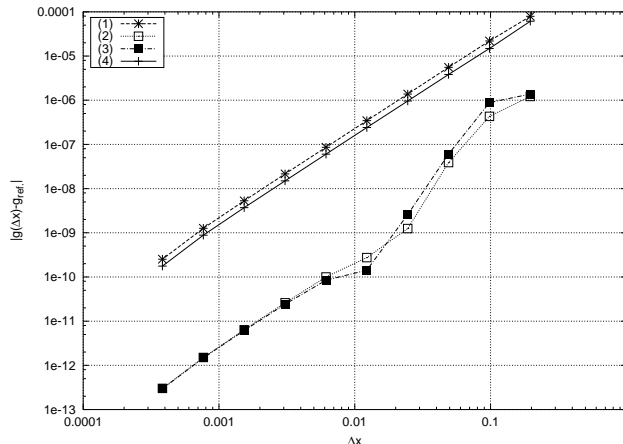


Figure 7: Absolute error between perturbed simulation at specified Δx vs. simulation at $\Delta x = \frac{\pi}{2^{14}}$ for Courant number $\alpha = 0.50$. Perturbation is a moving sinusoidal wave with wave number $k = 16$ and initial amplitude $A_0 = 10^{-6}$. Legend is (1) = ICN, (2) = RK3, (3) = RK4 and (4) = CFLN.

We see from the figure that the perturbed solution is converging for all schemes. For higher resolutions the convergence is at least second order. Similar convergence rates are seen for analogous simulations with other base solutions.

Figure 8 shows the ratio of the final amplitude (A_t) of a perturbation at time $t = \pi/4$ to its initial amplitude ($A_0 = 10^{-6}$) as a function of the resolution of the perturbed wave for simulations with base solution 2.3 with $C_1 = 10$ and $C_2 = -1$. Courant $\alpha = 0.50$ and $\Delta x = \frac{\pi}{2^{13}}$ was used in all simulations. The rightmost data point corresponds to a perturbation being at the Nyquist frequency. The analytical prediction is that

$$A_{t=\pi/4}/A(0) = \exp - \frac{C_2 \cdot t}{2C_1 - 2C_2 \cdot t} \approx 1.0435$$

according to (2.12). This prediction is also shown on the figure as line (0).

From this figure we see that at high resolutions all schemes produce the same growth of amplitude of perturbations, which is in agreement with the analytical prediction. As the resolution decreases the results for all schemes for all schemes begin to deviate from the analytical value. Among the method of lines schemes, the RK4 is the most accurate and is able to reproduce the correct behavior of the perturbation up to the resolution of 16 grid points per wavelength. CFLN also requires only 16 grid points per wavelength to reproduce the correct behavior. The other two schemes requires from 32 to 64 grid points per wavelength. The major difference between the CFLN and the method of lines schemes is that at low resolutions, CFLN is amplifying the perturbations more than it should according to the analytical predictions, whereas the method of lines schemes are damping. The RK4 is the least damping and the most accurate of these schemes. The behavior of the schemes at low resolutions is fully consistent with the results of the Von Neumann stability analysis, presented in section 4.1. According to that analysis the

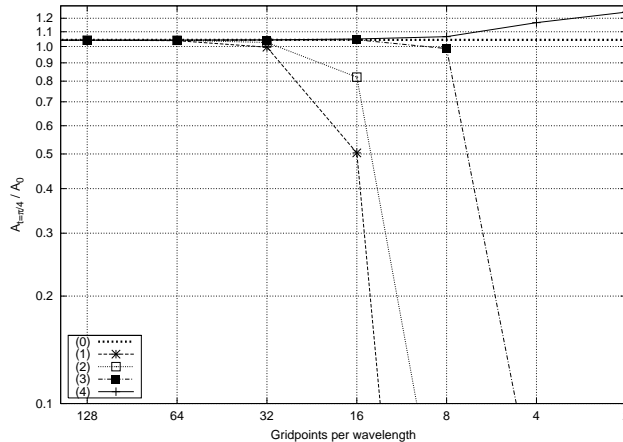


Figure 8: A_t/A_0 of sinusoidal perturbation at $t = \pi/4$ for base solution (2.3) versus various wave numbers for a fixed $\Delta x = \frac{\pi}{2^{13}}$ and $\alpha = 0.50$. Legend is (0) = Analytic prediction, (1) = ICN, (2) = RK3, (3) = RK4 and (4) = CFLN.

CFLN scheme must be amplifying at all wavelengths whereas the method of lines schemes must be damping.

6 Discussion and conclusion

In this paper we studied the properties of four numerical schemes, CFLN, ICN, RK3 and RK4, applied to a non-linear scalar wave equation (2.1). This equation has a number of non-trivial analytic solutions whose properties, including stability, were studied and summarized in section 2. We carried out the Von Neumann stability analysis of the schemes and studied their phase and amplitude errors. Finally we carried out numerical experiments and compared the results of those experiments with the perturbation analysis of the equation and the Von Neumann stability analysis of the schemes.

We find that all four schemes presented in this paper are stable and converge with the second order accuracy. The stability range for the schemes were determined and are presented in table 3. Those ranges are valid for both linear and non-linear solutions.

For non-linear schemes we checked that the amplification factor $|\lambda|$ is less than $1 + O(\Delta t)$ for sufficiently small Δt .

With respect to the dissipation errors, we find that the CFLN has the least amount of dissipation. The ICN scheme has the largest dissipation errors. The RK3 and RK4 are intermediate. For the method of lines schemes we find that damping is behaving non-monotonically with the increase of the Courant number.

With respect to phase errors, the schemes can be arranged in the sequence CFLN RK3, RK4

and ICN, with the CFLN having the least amount of errors and ICN having the largest.

We find that CFLN scheme requires the least amount of operations per time step, whereas the RK4 requires the largest amount.

Ideally a numerical scheme is preferable which has the minimal phase and amplitude errors, and is computationally inexpensive. It is also of practical importance to have a scheme which will damp the high frequency perturbations at and close to the Nyquist frequency. Otherwise truncation errors at the highest frequency will remain within the computational domain, may be amplified and may eventually spoil the solution. None of the schemes discussed in this paper satisfy all those criteria. We think that the RK4 scheme should be preferred to other schemes because of its damping properties at the Nyquist frequency and the minimal amount of errors consistent with this property. On the other hand, the amount of dissipation in the RK4 scheme is dependent upon Courant number and is not controllable. If not for the damping properties, the CFLN scheme is the most accurate and cost effective. It would be of great interest to develop a version of this scheme with a controllable filter, for damping the minimum amount of perturbations at a narrow range of frequencies near the Nyquist frequency.

This work was supported in part by Danmarks Grundforskningsfond through its support for establishment of the Theoretical Astrophysics Center and by the Danish SNF Grant 21-03-0336. We thank A. Doroshkevich and R. Takahashi for useful discussions. The authors thank Caltech for hospitality during their visits.

References

- [1] M. Alcubierre et. al., (2000) *Towards a Stable Numerical Evolution of Strongly Gravitating Systems in General Relativity: The Conformal Treatments*, Phys.Rev. D62:044034.
- [2] S.A. Teukolsky, (2000), *Stability of the iterated Crank-Nicholson method in numerical relativity*, Phys. Rev., D61:087501.
- [3] A. Khokhlov, I.D. Novikov, *A scalar hyperbolic equation with GR-type non-linearity*, gr-qc/0303063, accepted for publication in International Journal of Modern Physics.
- [4] B. Gustafsson, H. O. Kreiss and J. Olinger, (1995), *Time dependent problems and difference methods*, Wiley, New York.
- [5] R. Courant, K. O. Friedrichs and H. Levy, (1928), Math. Ann., 100:32.
- [6] J. Crank and P. Nicolson, (1947), *A practical method for numerical integration of solutions of partial differential equations of heat-conduction type*, Proc. Cambridge Philos. Soc., vol. 43, p. 50, 1947.
- [7] R. D. Richtmeyer and K.W. Morton, (1967), *Difference Methods for Initial-Value Problems*, 2nd ed., New York:Wiley-Interscience.
- [8] M. Abramowitz and I .A. Stegun, (1965), *Handbook of Mathematical functions*, Dover.
- [9] M. Miller, (2000), *On the Numerical Stability of the Einstein Equations*, gr-gc/0008017.